# Archaeal lipid-inferred paleohydrology and paleotemperature of Lake Chenghai during the Pleistocene-Holocene transition

Weiwei Sun [a], Enlou Zhang [a, b, *], Jie Chang [a], James Shulmeister [c, d], Michael I. Bird [e, f], Cheng Zhao [a, b], Qingfeng Jiang [g], Ji Shen [a]

[a] State Key Laboratory of Lake Science and Environment, Nanjing Institute of Geography and Limnology, Chinese Academy of Sciences, Nanjing 210008, China

[b] Center for Excellence in Quaternary Science and Global Change, Chinese Academy of Science, Xian 710061, China

[c] School of Earth and Environmental Sciences, The University of Queensland, St Lucia, Brisbane, Qld, 4072, Australia

[d] School of Earth and Environment, University of Canterbury, Private Bag 4800, Christchurch, New Zealand

[e] ARC Centre of Excellence for Australian Biodiversity and Heritage, James Cook University, PO Box 6811, Cairns, Queensland, 4870, Australia

[f] College of Science and Engineering, James Cook University, PO Box 6811, Cairns, Queensland, 4870, Australia

[g] School of Geography Sciences, Nantong University, Nantong, 226007, China

* Corresponding authors. elzhang@niglas.ac.cn. State Key Laboratory of Lake Science and Environment, Nanjing Institute of Geography and Limnology, Chinese Academy of Sciences, Nanjing 210008, China

## ABSTRACT

Over the past decades, paleoenvironmental studies in the Indian Summer Monsoon (ISM) region have mainly focused on precipitation change, with few published terrestrial temperature records from the region. We analyzed the distribution of isoprenoid glycerol dialkyl glycerol tetraethers (isoGDGTs) in the sediments of Lake Chenghai in southwest China across the Pleistocene–Holocene transition, to extract both regional hydrological and temperature signals for this important transition period. Lake-level was reconstructed from the relative abundance of crenarchaeol in isoGDGTs (%cren) and the crenarchaeol'/crenarchaeol ratio. The %cren-inferred lake-level identified a single lowstand (15.4-14.4 cal ka BP), while the crenarchaeol'/crenarchaeol ratio suggests relatively lower lake-level between 15.4-14.4 cal ka BP and 12.5-11.7 cal ka BP, corresponding to periods of weakened ISM during the Heinrich 1 and Younger Dryas cold event. A filtered TetraEther indeX consisting of 86 carbon atoms ($TEX_{86}$ index) revealed that lake surface temperature was similar to present-day values during the last deglacial period, and suggests a substantial warming of ~4 ℃ from the early Holocene to the mid-Holocene. Our paleotemperature record is generally consistent with other records in southwest China, suggesting that the distribution of isoGDGTs in Lake Chenghai sediments has potential for quantitative paleotemperature reconstruction.



**Keywords**: Quantitative temperature reconstruction; Lake-level; $TEX_{86}$; Isoprenoid GDGTs; Lacustrine sediment

## 1. Introduction

Precipitation variation in the Indian summer monsoon (ISM) region has a great threat to ecosystem function, water availability and economic security across the region (Sinha et al., 2011; Sinha et al., 2015; Ljungqvist et al., 2016). This has stimulated growing scientific interest in understanding the underlying forcing mechanisms behind climate variability in the ISM region on a range of time-scales, in order to better predict future monsoonal variations. Over the past two decades, climate evolution in the ISM region since the Last Glacial Maximum has been reconstructed from various paleoclimatic archives, including speleothems, and marine/lacustrine sediments (Dykoski et al., 2005; Rashid et al., 2007; Govil and Divakar Naidu, 2011; Saraswat et al., 2013; Contreras-Rosales et al., 2014; Wang et al., 2014b; Dutt et al., 2015; Wu et al., 2015; Kathayat et al., 2016; Zhang et al., 2017a, 2017b; Li et al., 2018; Zhang et al., 2018; Sun et al., 2019; Zhang et al., 2019). These studies provide evidence of changes in ISM precipitation on orbital- and millennial time-scales, with a weakened ISM occurring during cold events, and strengthened ISM occurring during warm intervals.

In addition to precipitation, temperature is an important climatic factor, due to its significant effects on evaporation and regional hydrological cycle. There remains a lack of quantitative reconstructions of terrestrial temperature from the ISM region (Shen et al., 2006; Zhang et al., 2017a; Wu et al., 2018; Feng et al., 2019; Ning et al., 2019; Tian et al., 2019; Zhang et al., 2019). During the last deglaciation-Holocene transition, the climate of high latitudes in the Northern Hemisphere is punctuated by three abrupt, millennial-scale events: the Heinrich 1 (H1) cold event, the Bølling/Allerød (BA) warm period and the Younger Dryas (YD) cooling (Alley and Clark, 1999). These intervals are attributed to a variety of mechanisms including changes to orbitally-controlled insolation, ice sheet extent, oceanic circulation and atmospheric greenhouse concentrations (Alley and Clark, 1999). The recent quantitative summer temperature proxy based on pollen and chironomids from southwest China has been developed to address the response of long-term temperature

to the high latitude climate changes (Zhang et al., 2017 and 2019; Wu et al., 2018). However, the magnitude of these temperature variations is not consistent, and further studies are required.

Glycerol dialkyl glycerol tetraethers (GDGTs) have been widely used for the quantitative reconstruction of terrestrial paleotemperature during the Quaternary due to the fact that they are ubiquitous in soils and lacustrine sediments (Blaga et al., 2013; Wang et al., 2017b; Zheng et al., 2018; Ning et al., 2019; Tian et al., 2019). Isoprenoid GDGTs (isoGDGTs), comprising acyclic or ring-containing isoprenoidal biphytanyl carbon chains, are a suit of membrane lipids produced by some species of archaea, such as Euryarchaeota, Crenarchaoeota and Thaumarchaeota (Schouten et al., 2013). IsoGDGTs containing 0 to 3 cyclopentane moieties (isoGDGTs 0–3, Fig. S1) are common isoGDGTs with a large range of biological sources (Schouten et al., 2013). For example, Thaumarchaeota were the dominant biological source of GDGT-0 in Lake Lucerne from Switzerland (Blaga et al., 2011); while GDGT-0 in Lake Challa surface sediments might predominantly derive from archaea residing in the deeper, anoxic water column, such as group 1.2 and marine benthic group C group of the Crenarchaeota, and the Halobacteriales of the Euryarchaota (Sinninghe Damsté et al., 2009); and methanogenic and methanotrophic archaea can also be two important sources of GDGT-0 within the water column and sediment (Blaga et al., 2009; Powers et al., 2010). In contrast, crenarchaeol and its regioisomer, crenarchaeol' (Fig. S1), are considered to be produced specifically by mesophilic Thaumarchaeota in aquatic environments (Schouten et al., 2002; Blaga et al., 2009; Kim et al., 2010; Powers et al., 2010; Schouten et al., 2013). On this basis, the ratio of GDGT-0/crenarchaeol has been proposed to evaluate the influence of Thaumarchaeota on the distribution of isoGDGTs in lacustrine sediments, and the ratio typically varies between 0.2 and 2 in Thaumarchaeota (Schouten et al., 2002; Blaga et al., 2009).

Thaumarchaeota have a physiological mechanism to increase the weighted average number of cyclopentane rings in their membrane lipids with growth temperature (Schouten et al., 2002). Thus the TetraEther indeX consisting of 86

carbon atoms ($TEX_{86}$ index), which represents the relative number of cyclopentane moieties in isoGDGT molecules derived from aquatic Thaumarchaeota, has great potential for use as a paleotemperature proxy in the marine environment and large lakes (Tierney et al., 2008; Berke et al., 2012; Blaga et al., 2013; Wang et al., 2015). However, the index may not be a reliable proxy for past temperature in small lakes due to substantial amounts of soil and/or methanogenic archaea isoGDGTs identified in the same lacustrine sediment and also due to variability in the depth of isoGDGT production in aquatic ecosystems (Blaga et al., 2009; Powers et al., 2010; Sinninghe Damsté et al., 2012a).

It has also been shown that crenarchaeol' is only present in low abundance in most Thaumarchaeota except for the group I.1b Thaumarchaeota, where it is one of the major isoGDGTs (Kim et al., 2012; Sinninghe Damsté et al., 2012b). The crenarchaeol'/crenarchaeol ratios for enrichment cultures of group I.1a aquatic Thaumarchaeota are typically 0.01-0.04, however, for group I.1b Thaumarchaeota enriched from soils the crenarchaeol'/crenarchaeol ratios are around 0.21 and substantially higher (Pitcher et al., 2011; Sinninghe Damsté et al., 2012a). In addition, a likely Group I.1b Thaumarchaeota population inhabiting the subsurface water column near the anoxic-suboxic boundary was found in Lake Malawi, but the total production of isoGDGTs by this group appears to be much lower than the surface-dwelling Thaumarchaeota (Meegan Kumar et al., 2019).

In addition, aquatic Thaumarchaeota are nitrifers, that prefer to live above the oxycline of relatively deep lakes, as has been observed by a range of lipid biomarker and DNA based investigations of vertical changes in archaea communities in lake water columns (Sinninghe Damsté et al., 2009; Blaga et al., 2011; Schouten et al., 2012; Buckles et al., 2013; Meegan Kumar et al., 2019). Some Thaumarchaeota are thought to be suppressed by a high light level, which consequently might also inhibit their ability to thrive near the surface of lakes (Schouten et al., 2013). Further, Thaumarchaeota are chemoautotrophic and thrive predominantly near the oxycline in stratified lakes, mainly due to the release of ammonia derived from descending

particulate organic matter that is recycled primarily by photoautotrophs or heterotrophs in the photic zone (Tierney et al., 2010). Consequently, the proportion of crenarchaeol in isoGDGTs (cren%) has been suggested as lake-level proxy (Wang et al., 2014a; Wang et al., 2017a; Wang et al., 2019). However, it has also been suggested that mixing of the water column will be much more frequent at lowstand conditions, and therefore periodically or permanently oxic, high nutrient availability water and enhanced nitrogen cycling would be likely to result in a relatively higher production of crenarchaeol (Filippi and Talbot, 2005; Sinninghe Damsté et al., 2012).

In this study, we present an isoGDGT record spanning the last deglacial-Holocene transition from Lake Chenghai in the southwest China. Our stable oxygen isotope ($\delta^{18}O$) record of authigenic carbonates from Lake Chenghai previously revealed that drought events occurred from 15.6 to 14.4 cal ka BP and 12.5 to 11.7 cal ka BP corresponding to the H 1 and YD event (Sun et al., 2019). The present study aims were to (1) identify sources of isoGDGTs in Lake Chenghai sediments and their linkage, if any, with lake-level variation; (2) test the reliability of isoGDGT-based proxies as temperature indicators, by comparing our results with other paleoenvironmental records from adjacent areas, and explore the possible mechanisms driving temperature variations during the last deglaciation-Holocene transition in southwestern China.

## 2. Materials and methods

### *2.1. Regional setting*

Lake Chenghai (26°27′-26°38′N, 100°38′-100°41′E, Fig. 1A) is a tectonic lake located in the northwestern part of Yunnan Province (Wang and Dou, 1998). The current water surface elevation is ~1500 m above sea level (a.s.l.), and the maximum water depth is ~35 m. The lake is hydrologically closed at present, with a surface area of ~77 $km^2$ and a catchment of ~318 $km^2$ (Wu et al., 2004). However, Lake Chenghai was linked to the Jinsha River via the Haikou River before a dam at an elevation of

~1540 m a.s.l. was constructed on its southern side at ~0.3 cal ka BP (Wang and Dou, 1998). The annual mean lake surface temperature (LST) is ~16 ℃ (Wan et al., 2005). In summer, the lake becomes thermally stratified, with the thermocline at between 10 to 20 m (Fig. 1C, Lu, 2018). Despite a relatively large catchment, the lake level is mainly maintained by direct precipitation and groundwater, with a total dissolved solid load of ~1‰ and pH of ~8 (Wan et al., 2005). The lake is eutrophic with a total phosphate concentration of 0.05 mg/L, and total nitrogen concentration of 0.89 mg/L (Li et al., 2019). Topsoil types are lateritic red earths and mountain red brown soils in the catchment (Wang and Dou, 1998). The Lake Chenghai region is mainly affected by a warm-humid monsoonal airflow from the tropical Indian Ocean from June to September, and by the southern branch of the Northern Hemisphere westerly jet between October and May (Wang and Dou, 1998). The mean annual temperature is ~14 ℃, the mean annual precipitation is ~660 mm with 80% falling between June and September (the Yongsheng meteorological station 26.68 ℃N, 100.75 ℃E; elevation of 2130 m a.s.l.).

*2.2. Sampling and dating*

In summer 2016, an 874-cm-long sediment core (CH2016) was retrieved using a UWITEC coring platform system with a percussion corer in 30 m of water depth (26°33′29.4″N, 100°39′6.7″E). Each section of the core was split lengthways, photographed and then sectioned at a 1-cm interval in the laboratory; the samples stored at 4 ℃ until analysis. The chronology was established using accelerator mass spectrometry (AMS) $^{14}$C dating of eight terrestrial plant macrofossils and charcoal (Sun et al., 2019). The radiocarbon analyses were performed at the Beta Analytic Radiocarbon Dating Laboratory in Miami, USA. The age model was developed utilizing Bacon, implemented in R 3.1.0 at 5-cm intervals (Blaauw and Andres Christen, 2011; R Development Core Team, 2013). All AMS $^{14}$C dates were calibrated to calendar years before present (0 BP =1950) using the program Calib 7.1 and the IntCal13 calibration data set (Reimer et al., 2013). The basal mean weighted age is ~15.6 cal ka BP (Fig. 2, Sun et al., 2019).

196 *2.3. Lipid extraction and analysis*

197 A total of 102 freeze-dried samples at 4-cm interval were collected for GDGT
198 analysis over the last deglaciation-Holocene transition. The sampling resolution was
199 increased to 1-cm between 792- 806 cm, due to the low sedimentation rate observed
200 in this section. In addition, seven surface (the top 2 cm) sediments covering the whole
201 lake sampled in 2014 were also analyzed. Lipid extraction was undertaken according
202 to the procedures in Feng et al (2019). A ~4 g aliquot of each sample was extracted
203 ultrasonically (4 times) with a mixture of dichloromethane and methanol (9:1, v/v).
204 The supernatants were condensed and saponified at room temperature for 12 h with a
205 1 M KOH/methanol solution. The neutral fractions were then separated into apolar
206 and polar fractions on a silica gel column, using *n*-hexane and methanol, respectively.
207 The polar fraction containing the GDGTs was concentrated and filtered through 0.45
208 μm polytetrafluoroethylene syringe filters using *n*-hexane/ isopropanol (99:1 v/v), and
209 then dried under $N_2$.

210 GDGTs were analyzed using an Agilent 1260 series high performance liquid
211 chromatography-atmospheric pressure chemical ionization-mass spectrometer
212 (HPLC-APCI-MS), following the procedure of Yang et al. (2015) at the Institute of
213 Tibetan Plateau Research, Chinese Academy of Sciences. Briefly, the GDGTs were
214 separated using three silica columns in tandem (100 mm× 2.1 mm, 1.9 μm; Thermo
215 Fisher Scientific, U.S.A.), maintained at 40 ℃. The elution gradients were 84%
216 *n*-hexane (A): 16% ethyl acetate (B) for 5 min, 84/16 to 82/18 A/B for another 60 min,
217 then to 100% B for 21 min and kept for 4 min, followed by a return to 84/16 A/B for
218 30 min. The total flow rate of pump A and pump B was maintained at 0.2 ml/min. The
219 APCI-MS conditions were: vaporizer pressure 60 psi, vaporizer temperature 400 ℃,
220 drying gas flow 6 L/min and temperature 200 ℃, capillary voltage 3500 V and corona
221 current 5 μA (~3200 V). Selected ion monitoring (SIM) mode was performed to target
222 specific *m/z* values for each GDGT compound, including 1302 (GDGT-0), 1300
223 (GDGT-1), 1298 (GDGT-2), 1296 (GDGT-3), and 1292 (crenarchaeol and
224 crenarchaeol'). The results are presented as the fractional of the sum of the isoGDGTs

based on the integration of the peak areas of the $[M+H]^+$ ions.

*2.4. Index calculation and temperature reconstruction*

The percentage of each isoGDGT (X) was calculated according to the following equation:

$$\%X = X / (GDGT\text{-}0 + GDGT\text{-}1 + GDGT\text{-}2 + GDGT\text{-}3 + crenarchaeol + crenarchaeol') \quad (1)$$

The $TEX_{86}$ index was defined by Schouten et al. (2002) as follows:

$$TEX_{86} = (GDGT\text{-}2 + GDGT\text{-}3 + crenarchaeol') / (GDGT\text{-}1 + GDGT\text{-}2 + GDGT\text{-}3 + crenarchaeol') \quad (2)$$

$TEX_{86}$-inferred LST was calculated using the global lake calibration of Castañeda and Schouten (2015):

$$LST = 49.03 \times TEX_{86} - 10.99 \quad (r^2 = 0.88, n=16, RMSE = 3.1\ ℃) \quad (3)$$

## 3. Results

The isoGDGT compositions varied greatly in Lake Chenghai sediments. As illustrated in Fig. 3, GDGT-0 is the most abundant isoGDGT composition of the surface sediments. The relative abundance of GDGT-0 (%GDGT-0) ranged from 71.6-94.4 with a mean of 89.2%, the %cren values varied from 3.8- 18.1% with a mean of 7.6%. The ratios of GDGT-0/crenarchaeol were from 4.0-24.5 with a mean of 15.5. The average values of GDGT-1, GDGT-2 and GDGT-3 relative abundance were 1.2, 1.1 and 1.4%, respectively. The crenarchaeol's regioisomer, crenarchaeol', occurred in only low abundance, close to the detection limit, and therefore $TEX_{86}$ values could not be calculated for these surface sediments.

The %cren values ranged between 2.4-61.3% with a mean of 52.4% in the core CH2016. The %cren values were relatively low and highly variable during 15.4-14.4 cal ka BP, ranging between 1.8-32.0%, with a mean of 11.6%. By contrast, the values

were relatively stable during 14.4-7.0 cal ka BP, ranging between 41.8-61.3% with a mean of 58.3%. The relative abundances of crenarchaeol' had a mean of 1.7%. The ratios of crenarchaeol'/crenarchaeol were highly variable during 15.4-14.4 cal ka BP with a mean of 0.07. After this time, the values gradually decrease during 14.4-11.7 cal ka BP time interval with a minor increase between 12.5-11.7 cal ka BP, where the ratio averaged 0.05. The crenarchaeol'/crenarchaeol ratios were generally stable and fluctuated around 0.03 during the period 11.8-7.0 cal ka BP.

The relative abundances of GDGT-0 (%GDGT-0) showed a significant negative correlation with the %cren in the core CH2016 (r= 0.99, $p< 0.001$). The %GDGT-0 values had a mean of 74.0% between 15.4-14.4 cal ka BP and a mean of 19.6% during the 14.4-7.0 cal ka BP interval. The values of GDGT-0/crenarchaeol were generally >2 during the period 15.4-14.4 cal ka BP, ranging from 1.4-49.9 with a mean of 16.7, and all <2 from 14.4-7.0 cal ka BP. The relative abundance of GDGT-1, GDGD-2 and GDGT-3 were generally low in the sediments, with means of 8.9, 9.2, and 1.3, respectively.

The $TEX_{86}$ values were also highly variable during 15.4-14.4 cal ka BP period, ranging between 0.36-0.68 with a mean of 0.54. Thereafter, the values generally followed an increasing trend, ranging between 0.49-0.63 with a mean of 0.58.

## 4. Discussion

### *4.1. Provenance of isoGDGTs*

In order to evaluate the potential sources of isoGDGTs in Lake Chenghai sediments, we plotted a ternary diagram to compare the distribution patterns of GDGT-0, crenarchaeol, and the sum of GDGT-1, GDGT-2, GDGT-3, and crenarchaeol' ('$TEX_{86}$' GDGT) among our samples, previously published Chinese soils and global marine sediments compiled by Yao et al. (2019), along with previously published Chinese lacustrine surface sediments results (Günther et al., 2014; Dang et al., 2016; Hu et al., 2016; Li et al., 2016, 2019; Yao et al., 2019; Wang

et al., 2020). In Lake Chenghai surface sediments, GDGT-0 is the predominant component among the isoGDGTs, consistent with most previous studies of lacustrine sediments (Blaga et al., 2009; Dang et al., 2016; Li et al., 2019; Yao et al., 2019; Wang et al., 2020). For example, GDGT-0 can account for more than 90% of total isoGDGTs in shallow lake surface sediments from East China (Dang et al., 2016); ~80% in saline pond surface sediments from northeast China (Li et al., 2019), and ~54% in surface sediments from the Qinghai-Tibetan Plateau (Wang et al., 2020). The values of GDGT-0/cren >2 in Lake Chenghai surface sediment suggest non-thaumarchaeotal isoGDGTs are also likely to be an important source in this lake system. The distribution of isoGDGTs between Chinese lacustrine surface sediments and soils were similar, and both were generally higher than that in global marine sediments and Thaumarchaeota. This line of evidence also suggests that the surface sediments could contain a significant contribution of soil isoGDGTs input (Li et al., 2016; Li et al., 2019).

The distribution of isoGDGT in Lake Chenghai sediment from 15.4-14.4 cal ka BP was similar to that of the surface sediments, suggesting a substantial contribution of non-thaumarchaeota during this period. However, the relative abundance of GDGT-0 significantly decreased and %cren increased in Lake Chenghai sediments from 14.4-7.0 cal ka BP. The plots generally overlapped with those of global marine sediments and Thaumarchaeota in the ternary diagram during this period, indicating that Thaumarchaeota dominated the archaea community in Lake Chenghai during the late glacial period and the early Holocene. The observed down-core changes in crenarchaeol'/crenarchaeol ratios may be due to relatively high contributions of group I.1b Thaumarchaeota from soils during the period 15.4-11.8 cal ka BP, and that these dominate the contributions of isoGDGTs derived from aquatic group I.1a Thaumarchaeota during the period from 11.8-7.0 cal ka BP.

### *4.2. Assessment of isoGDGT-based lake-level proxy*

The environmental implication of %cren at Lake Chenghai during the period from the last deglaciation to the early Holocene is illustrated in Fig. 5. The relatively

low %cren values during 15.4-14.4 cal ka BP is consistent in timing with the $\delta^{18}O$ record of authigenic carbonates derived from the same core (Fig. 4e, Sun et al., 2019), speleothem $\delta^{18}O$ records from Mawmluh Cave and Bittoo Cave in north India (Fig. 4f, Dutt et al., 2015; Kathayat et al., 2016), and Donnge Cave in southwest China (Dykoski et al., 2005), which all record a substantial positive shift in $\delta^{18}O$ values at that time. Speleothem $\delta^{18}O$ records in the ISM region are used as a rainfall amount proxy, tracking changes in monsoon intensity (Dykoski et al., 2005; Cheng et al., 2012; Dutt et al., 2015). This suggests that the Thaumarchaeota were mainly suppressed by non-thaumarchaeotal archaea. Thus the abrupt increase in %cren values at 14.4 cal ka BP is suggested to represent a lowstand of Lake Chenghai during 15.4-14.4 cal ka BP, and a highstand period thereafter.

The interpretation of %cren contradicts the case for Lake Challa, but is consistent with that for Lake Qinghai in northwest China (Sinninghe Damsté et al., 2012; Wang et al., 2014). This difference is possibly due to the different response of Thaumarchaeota in the two types of lakes because of the mixing regime. For the small and deep Lake Challa, there is never complete mixing due to the stable stratification of the warmer water column and the lack of seasonality (Sinninghe Damsté et al., 2009). Below the oxycline nitrate levels are high, more substantial mixing regenerates more nutrients to the surface waters, resulting a relatively higher production of crenarchaeol (Sinninghe Damsté et al., 2012). In contrast, Lake Chenghai and Lake Qinghai are seasonal mixing lakes, and the vertical change of nutrients may be relatively small in the lake water. In addition, the low lake level during the H1 event was associated with a weakened ISM, and less terrestrial nutrient input due to less runoff would likely suppress the growth of Thaumarchaeota and reduce the production of crenarchaeol.

Low lake-levels and a weakened ISM during the H1 cold event are also observed in several previous paleolimnolgical studies from the Yunnan Plateau, within the uncertainties of the age model. Diatom and grain-size records from Lake Tengchongqinghai show a significant decrease in acidophilous diatom species and an

increase in the grain-size of mineral particles from 18.5 to 15.0 cal ka BP, suggesting that the climate was dry and the ISM was at its weakest since the last deglaciation (Fig. 4g, Zhang et al., 2017b; Li et al., 2018). Similarly, an increase in >30 μm grain-size particles in the late glacial sediments from Lake Xingyun reflects a period of abrupt weakening of the ISM during the H1 cold event because of reduced lake level (Wu et al., 2015). In Lake Lugu, the loss of the planktonic diatoms and a switch to small *Fragilaria* spp. suggests a weaker stratification from 24.5 to 14.5 cal ka BP, which might also correspond to low lake-level at that time (Wang et al., 2014b). In addition, there is a peak of cren% centered at ~15.2 cal ka BP, suggesting a centennial high lake-level and strengthened ISM period, which was not identified in a previous $\delta^{18}O$ record of authigenic carbonates (Sun et al., 2019). However, the strengthened ISM event at ~15.2 cal ka BP was clearly recorded by speleothem $\delta^{18}O$ record from Dongge Cave in southwest China (Dykoski et al., 2005).

Lake levels inferred from %cren do not show a lowstand during the YD (~12.8-11.7 cal ka BP), which is generally recognised as a period of low rainfall due to the weakening of the ISM (Dutt et al., 2015; Dykoski et al., 2005; Kathayat et al., 2016; Sun et al., 2019). In contrast, a low lake-level signal is observed in the $\delta^{18}O$ record of authigenic carbonates from Lake Chenghai (Sun et al., 2019). In addition, increased lake water alkalinity and decreased lake-level are also recorded in the diatom and grain-size proxy records between 12.8-11.1 cal ka BP of Lake Tengchongqinghai (Fig. 4g, Zhang et al., 2017b; Li et al., 2018). The inferred high lake levels during the YD which is inconsistent with a weakened ISM inferred from other proxies, might be due to the erosion of soil organic matter into the lake during this period (Wang et al., 2019). The crenarchaeol are relatively abundant in topsoils from southwest China, and the influence of soil input should be more significant at times of drier conditions (Yang et al., 2019). It is also worth noting that the crenarchaeol'/crenarchaeol ratios were not only relatively higher during the H1 cold event, but also showed a minor reversal during the YD cold event. These results are consistent with group I.1b Thaumarchaeota being an important source of isoGDGTs

366 in small lakes and in the nearshore areas of large lakes (Wang et al., 2019).

367 Another possibility for the unexpected H1 and YD lake level is the sensitivity of
368 the proxy to lake-level variation in the case of Lake Chenghai. The $\delta^{18}O$ record of
369 authigenic carbonates from Lake Chenghai and speleothem $\delta^{18}O$ records in the ISM
370 region suggest that the weakening of the ISM during the YD was less marked than
371 that occurring during the H1 event, in turn suggesting that lake-levels in southwest
372 China may have been higher during the YD than the H1 event (Dykoski et al., 2005;
373 Dutt et al., 2015; Kathayat et al., 2016; Sun et al., 2019; Zhang et al., 2019). For
374 the %cren proxy, we note that the values are correlated to the logarithm of depth,
375 suggesting that %cren may be less sensitive to water depth variation when the
376 lake-level is relatively high, and more sensitive to water depth variation when the
377 lake-level is lower (Wang et al., 2019).

378 *4.3. Warming in the last deglaciation-Holocene transition*

379 The application of the $TEX_{86}$-based paleotemperature calibration depends
380 critically on the assumption that the isoGDGTs used for calculation of $TEX_{86}$ values
381 are mainly been derived from group I.1a in the water column (Blaga et al., 2009;
382 Castañeda and Schouten, 2011; Powers et al., 2010; Sinninghe Damsté et al., 2012a).
383 Since the influence of methanogenic archaea in the water column or archaea in the
384 catchment soils has been recognized as significant, Lake Chenghai sediments with
385 crenarchaeol'/crenarchaeol ratios >0.04 and/or GDGT-0/crenarchaeol ratio >2 are
386 excluded from the discussion below (Powers et al., 2010; Castañeda and Schouten,
387 2015). The ratio of branched GDGTs to isoGDGTs should be <0.5 if the
388 $TEX_{86}$-temperature calibration in previous studies, because the values are
389 generally >0.90 in soils, whereas values are close to zero for sediments from large
390 lakes (Hopmans et al., 2004; Weijers et al., 2006). However, recent studies of a wide
391 variety of lakes have suggested that at least some of the branched GDGTs can be
392 produced *in situ* in the lake (Blaga et al., 2010; Tierney et al., 2010; Pearson et al.,
393 2011; Hu et al., 2016; Dang et al., 2018; Russell et al., 2018). Therefore, *in situ*
394 production of branched GDGTs in Lake Chenghai cannot be fully excluded, and

therefore the ratio of branched GDGTs to isoGDGTs was ignored in this study. 74 samples remain that have isoGDGT distributions consistent with their dominant source being the aquatic Thaumarchaeota, most of these being from the time interval between 11.7-7.0 cal ka BP, and only a few from the last deglaciation (n= 6). Using Equation 4 developed by Castañeda and Schouten (2015) to calculate mean LST, yielded LST values from 14.3-20.1 ℃, with a mean of 18.0 ℃ (Fig. 5a).

LST was ~15.9 ℃ during the last deglacial period, a temperature approaching the 16 ℃ observed in the present Lake Chenghai. Considering the $TEX_{86}$-based LST transfer function has a RMSE of 3.1 ℃, this result is consistent with other recent reconstructed mean annual temperatures (MAT) in southwest China, which show the temperatures during the last deglaciation were generally similar to the present-day values. For example, the MAT inferred from branched GDGTs from Lake Tengchongqinghai in southwest China increased episodically from 12.0 ℃ to 14.0 ℃ between 19.2 and 10.0 cal ka BP, where the modern mean annual temperature is 14.7 ℃ (Tian et al., 2019). The $TEX_{86}$-based deglacial LST and MAT inferred from branched GDGTs from Nam Co in south Tibetan Plateau also reported values similar to the present-day (Günther et al., 2015). Furthermore, the July temperature derived from the chironomid record from Lake Tiancai, and pollen record from Lake Yidun showed that the climate during the deglacial period was ~2-3 ℃ cooler relative to today (Fig. 5b and c, Shen et al., 2006; Zhang et al., 2019). The amplitudes of reconstructed terrestrial temperatures change in the Indian summer monsoon region are generally consistent with those from the tropical Indian Ocean. Although estimates of sea surface temperatures in the Andaman Sea and Bay of Bengal were variable, the cooling ranged from 1-4 ℃ (Rashid et al., 2007; MARGO, 2009; Govil and Naidu, 2011; Gebregiorgis et al., 2016).

Following the YD cold event, LST ranged from 16.2 ℃ to 20.1 ℃ with an increasing trend, and the middle Holocene was generally warmer than the early Holocene (11.7- 8.2 cal ka BP). In the Indian summer monsoon region, the reconstructed MAT using the branched GDGT calibration from Lake Ximenglongtan

remained at ~12.5 ℃ from 9.4-7.6 cal ka BP, then experienced a rapid warming to 13.8 ℃ from 7.6-5.5 cal ka BP (Ning et al., 2019). Meanwhile, the branched GDGTs-MAT from Lake Tengchongqinghai also achieved its highest the highest value at around 7.1 cal ka BP (Tian et al., 2019). Similarly, summer temperatures reconstructed from Lake Tiancai and Lake Xingyun displayed lower values in the early Holocene when compared with that in the following millennium, though the amplitude of change is much lower (0.3 and 1.1 ℃ lower, respectively, Zhang et al., 2017a; Wu et al., 2018). The amplitude of the absolute scale of cooling and warming is of a lower magnitude in the chironomid, pollen and branched GDGT records as compared to the $TEX_{86}$-based reconstruction from Lake Chenghai. This may be due to the difference in the accuracy and precision of the proxy-based models, which also depend on the biological and seasonal sensitivity of the proxy, to constrain the absolute temperature values (Zhang et al., 2017).

We also noted that most of the lake records from not only the Indian summer monsoon region, but other parts of East Asia, show a thermal optimum at 8.0-7.0 cal ka BP (Ning et al., 2019). The summer isolation over the Northern Hemisphere, which is an important external forcing, was highest at ~11.0 cal ka BP, leading the temperature optimum in east and south Asia by 3-4 ka (Berger and Loutre, 1991). This indicates that additional feedback between solar insolation and internal processes, such as the persistence of remnants of the Northern Hemisphere ice-sheets during the early Holocene, should be considered in explaining this discrepancy (Ning et al., 2019). The Laurentide and Fennoscandian ice-sheets in the early Holocene enhanced surface albedo and reduced air temperature in the high latitudes, which likely led to enhanced westerlies transporting more cold air from the North Atlantic Ocean downward to the Indian monsoon affected regions of southwest China and north India through its south branch flow (Ning et al., 2019). In addition, the melting of ice-sheets is likely to have slowed down the Atlantic Meridional Overturning Circulation. This process could further result in a relatively weakened Indian summer monsoon, and a reduction in heat transported to the continent during the early

453 Holocene (Zhang et al., 2017a).

454

455 **5. Conclusions**

456 The record of isoGDGTs in the sediments of Lake Chenghai in southwest China
457 presented in this study allows us to test the ability of isoGDGT-based proxies in the
458 ISM region to reconstruct lake-level and temperature during the last
459 deglaciation-Holocene transition. The lake-level history inferred from %cren shows a
460 relative lowstand of Lake Chenghai during 15.4-14.4 cal ka BP, corresponding to a
461 period of weakened ISM during the H1 cold event. The indistinct signal of lake-level
462 variation during the YD cold event may be due to the group I.1b Thaumarchaeota
463 being an important source of isoGDGTs and consequently the lake level may have
464 been low during the YD cold event. After filtering for the influence of isoGDGTs
465 derived from soils in the surrounding catchment and non-thaumarchaeota, the $TEX_{86}$
466 paleothermometry revealed that the LST of Lake Chenghai was similar to the
467 present-day value during the last deglaciation. The lake also experienced a substantial
468 warming of ~4 ℃ from the early-Holocene to the mid-Holocene due to the melting of
469 the remnants of the continental ice-sheets in the Northern Hemisphere, which
470 gradually reduced winter westerly circulation. Overall, our results show that records
471 of isoGDGTs in Lake Chenghai sediments have potential for quantitative
472 paleotemperature reconstruction once potential underlying biases are properly
473 constrained.

474

475 **Data availability.**

476 All data in this study will be made available on request.

477 **Author contributions.**

478 W.S and E.Z designed the study, W.S performed the fieldwork and lab analysis. W.S
479 and E.Z led the writing of the paper, J.C, J. S, M.I.B, C.Z, Q.J and J.S contributed to

data interpretation and paper writing. All authors contributed to discussions and writing of the manuscript. The authors declare that they have no competing financial interests.

**Competing interests.**

The authors declare that they have no conflict of interest.

**Acknowledgments**

We thank Dr. R. Chen and D. Ning for field assistance and laboratory analysis. The research was supported by the found from the program of Global Change and Mitigation (2016YFA0600502), the National Natural Science Foundation of China (41702183 and 41572337), the Strategic Priority Research Program of Chinese Academy of Sciences (XDB40010200), and the fund from State Key Laboratory of Lake Science and Environment (2016SKL003).

**References**

Alley, R.B., Clark, P.U.: The deglaciation of the northern hemisphere: A global perspective. Annu. Rev. Earth Pl. Sc. 27, 149-182, DOI: 10.1146/annurev.earth.27.1.149, 1999.

Berger, A., Loutre, M.-F.: Insolation values for the climate of the last 10 million years. Quaternary. Sci. Rev. 10, 297-317: DOI: 10.1016/0277-3791(91)90033-Q, 1991.

Berke, M.A., Johnson, T.C., Werne, J.P., Schouten, S., Sinninghe Damsté, J.S.: A mid-Holocene thermal maximum at the end of the African Humid Period. Earth. Planet. Sc. Lett. 351-352, 95-104, DOI: 10.1016/j.epsl.2012.07.008, 2012.

Blaauw, M., Andres Christen, J.: Flexible paleoclimate age-depth models using an autoregressive gamma process. Bayesian. Anal. 6, 457-474, DOI: 10.1214/11-BA618, 2011.

Blaga, C.I., Reichart, G.-J., Heiri, O., Sinninghe Damsté, J.S.: Tetraether membrane lipid distributions in water-column particulate matter and sediments: a study of 47 European lakes along a north–south transect. J. Paleolimnol. 41, 523-540,

508 DOI: 10.1007/s10933-008-9242-2, 2009.
509 Blaga, C.I., Reichart, G.-J., Lotter, A.F., Anselmetti, F.S., Sinninghe Damsté, J.S.: A
510 $TEX_{86}$ lake record suggests simultaneous shifts in temperature in Central Europe
511 and Greenland during the last deglaciation. Geophys. Res. Lett. 40, 948-953,
512 DOI: 10.1002/grl.50181, 2013.
513 Blaga, C.I., Reichart, G.-J., Vissers, E.W., Lotter, A.F., Anselmetti, F.S., Sinninghe
514 Damsté, J.S.: Seasonal changes in glycerol dialkyl glycerol tetraether
515 concentrations and fluxes in a perialpine lake: Implications for the use of the
516 TEX86 and BIT proxies. Geochim. Cosmochim. Ac. 75, 6416-6428, DOI:
517 10.1016/j.gca.2011.08.016, 2011.
518 Blaga, C.I., Reichart, G.J., Schouten, S., Lotter, A.F., Werne, J.P., Kosten, S., Mazzeo,
519 N., Lacerot, G., Damste, J.S.S.: Branched glycerol dialkyl glycerol tetraethers in
520 lake sediments: Can they be used as temperature and pH proxies? Org. Geochem.
521 41, 1225-1234, DOI: 10.1016/j.orggeochem.2010.07.002, 2010.
522 Buckles, L.K., Villanueva, L., Weijers, J.W.H., Verschuren, D., Damsté, J.S.S.:
523 Linking isoprenoidal GDGT membrane lipid distributions with gene abundances
524 of ammonia-oxidizing Thaumarchaeota and uncultured crenarchaeotal groups in
525 the water column of a tropical lake (Lake Challa, East Africa). Environ.l
526 Microbiol. 15, 2445-2462, DOI: 10.1111/1462-2920.12118, 2013.
527 Carlson, A.E., LeGrande, A.N., Oppo, D.W., Came, R.E., Schmidt, G.A., Anslow, F.S.,
528 Licciardi, J.M., Obbink, E.A.: Rapid early Holocene deglaciation of the
529 Laurentide ice sheet. Nature Geosci. 1, 620-624, DOI: 10.1038/ngeo285, 2008.
530 Castañeda, I.S., Schouten, S.: A review of molecular organic proxies for examining
531 modern and ancient lacustrine environments. Quaternary. Sci. Rev. 30,
532 2851-2891, DOI: 10.1016/j.quascirev.2011.07.009, 2011.
533 Castañeda, I.S., Schouten, S.: Corrigendum to “A review of molecular organic proxies
534 for examining modern and ancient lacustrine environments” [Quat. Sci. Rev. 30
535 (2011) 2851–2891]. Quaternary. Sci. Rev. 125, 174-176, DOI:
536 10.1016/j.quascirev.2015.07.020, 2015.
537 Cheng, H., Sinha, A., Wang, X., Cruz, F.W., Edwards, R.L.: The Global

538 Paleomonsoon as seen through speleothem records from Asia and the Americas.
539 Clim. Dynam. 39, 1045-1062, DOI: 10.1007/s00382-012-1363-7, 2012.
540 Contreras-Rosales, L.A., Jennerjahn, T., Tharammal, T., Meyer, V., Lückge, A., Paul,
541 A., Schefuß, E.: Evolution of the Indian Summer Monsoon and terrestrial
542 vegetation in the Bengal region during the past 18 ka. Quaternary. Sci. Rev. 102,
543 133-148, DOI: 10.1016/j.quascirev.2014.08.010, 2014.
544 Dang, X., Ding, W., Yang, H., Pancost, R.D., Naafs, B.D.A., Xue, J., Lin, X., Lu, J.,
545 Xie, S.: Different temperature dependence of the bacterial brGDGT isomers in
546 35 Chinese lake sediments compared to that in soils. Org. Geochem., DOI:
547 10.1016/j.orggeochem.2018.02.008, 2018.
548 Dang, X.Y., Xue, J.T., Yang, H., Xie, S.C.: Environmental impacts on the distribution
549 of microbial tetraether lipids in Chinese lakes with contrasting pH: Implications
550 for lacustrine paleoenvironmental reconstructions. Sci. China. Earth. Sci. 59,
551 939-950, DOI: 10.1007/s11430-015-5234-z, 2016.
552 Dutt, S., Gupta, A.K., Clemens, S.C., Cheng, H., Singh, R.K., Kathayat, G., Edwards,
553 R.L.: Abrupt changes in Indian summer monsoon strength during 33,800 to
554 5500 years B.P. Geophys. Res. Lett. 42, 5526-5532, DOI:
555 10.1002/2015GL064015, 2015.
556 Dykoski, C.A., Edwards, R.L., Cheng, H., Yuan, D., Cai, Y., Zhang, M., Lin, Y., Qing,
557 J., An, Z., Revenaugh, J.: A high-resolution, absolute-dated Holocene and
558 deglacial Asian monsoon record from Dongge Cave, China. Earth. Planet. Sc.
559 Lett. 233, 71-86, DOI: 10.1016/j.epsl.2005.01.036, 2005.
560 Feng, X., Zhao, C., D'Andrea, W.J., Liang, J., Zhou, A., Shen, J.: Temperature
561 fluctuations during the Common Era in subtropical southwestern China inferred
562 from brGDGTs in a remote alpine lake. Earth. Planet. Sc. Lett. 510, 26-36, DOI:
563 10.1016/j.epsl.2018.12.028, 2019.
564 Filippi, M.L., Talbot, M.R.: The palaeolimnology of northern Lake Malawi over the
565 last 25 ka based upon the elemental and stable isotopic composition of
566 sedimentary organic matter. Quaternary. Sci. Rev. 24, 1303-1328, DOI:
567 10.1016/j.quascirev.2004.10.009, 2005.

568 Gebregiorgis, D., Hathorne, E.C., Sijinkumar, A.V., Nath, B.N., Nürnberg, D., Frank,
569 M.: South Asian summer monsoon variability during the last ~54 kyrs inferred
570 from surface water salinity and river runoff proxies. Quaternary. Sci. Rev. 138,
571 6-15, DOI: 10.1016/j.quascirev.2016.02.012, 2016.
572 Govil, P., Divakar Naidu, P.: Variations of Indian monsoon precipitation during the
573 last 32 kyr reflected in the surface hydrography of the Western Bay of Bengal.
574 Quaternary. Sci. Rev. 30, 3871-3879, DOI: 10.1016/j.quascirev.2011.10.004,
575 2011.
576 Günther, F., Thiele, A., Gleixner, G., Xu, B., Yao, T., Schouten, S.: Distribution of
577 bacterial and archaeal ether lipids in soils and surface sediments of Tibetan lakes:
578 Implications for GDGT-based proxies in saline high mountain lakes. Org.
579 Geochem. 67, 19-30, DOI: 10.1016/j.orggeochem.2013.11.014, 2014.
580 Günther, F., Witt, R., Schouten, S., Mäusbacher, R., Daut, G., Zhu, L., Xu, B., Yao, T.,
581 Gleixner, G.: Quaternary ecological responses and impacts of the Indian Ocean
582 Summer Monsoon at Nam Co, Southern Tibetan Plateau. Quaternary. Sci. Rev.
583 112, 66-77, 10.1016/j.quascirev.2015.01.023, 2015.
584 Hu, J., Zhou, H., Peng, P.a., Spiro, B.: Seasonal variability in concentrations and
585 fluxes of glycerol dialkyl glycerol tetraethers in Huguangyan Maar Lake, SE
586 China: Implications for the applicability of the MBT-CBT paleotemperature
587 proxy in lacustrine settings. Chem. Geol. 420, 200-212, DOI:
588 10.1016/j.chemgeo.2015.11.008, 2016.
589 Kathayat, G., Cheng, H., Sinha, A., Spötl, C., Edwards, R.L., Zhang, H., Li, X., Yi, L.,
590 Ning, Y., Cai, Y., Lui, W.L., Breitenbach, S.F.M.: Indian monsoon variability on
591 millennial-orbital timescales. Sci. Rep-UK. 6, DOI: 10.1038/srep24374, 2016.
592 Kim, J.-G., Jung, M.-Y., Park, S.-J., Rijpstra, W.I.C., Sinninghe Damsté, J.S., Madsen,
593 E.L., Min, D., Kim, J.-S., Kim, G.-J., Rhee, S.-K.: Cultivation of a highly
594 enriched ammonia-oxidizing archaeon of thaumarchaeotal group I.1b from an
595 agricultural soil. Environ. Microbiol. 14, 1528-1543, DOI:
596 10.1111/j.1462-2920.2012.02740.x, 2012.
597 Kim, J.-H., van der Meer, J., Schouten, S., Helmke, P., Willmott, V., Sangiorgi, F.,

598 Koç, N., Hopmans, E.C., Damsté, J.S.S.: New indices and calibrations derived
599 from the distribution of crenarchaeal isoprenoid tetraether lipids: Implications for
600 past sea surface temperature reconstructions. Geochim. Cosmochim. Ac. 74,
601 4639-4654, DOI: 10.1016/j.gca.2010.05.027, 2010.
602 Li, J.J., Pancost, R.D., Naafs, B.D.A., Yang, H., Zhao, C., Xie, S.C.: Distribution of
603 glycerol dialkyl glycerol tetraether (GDGT) lipids in a hypersaline lake system.
604 Org. Geochem. 99, 113-124, DOI: 10.1016/j.orggeochem.2016.06.007, 2016.
605 Li, J., Pancost, R.D., Naafs, B.D.A., Yang, H., Liu, D., Gong, L., Qiu, X., Xie, S.:
606 Multiple environmental and ecological controls on archaeal ether lipid
607 distributions in saline ponds. Chem. Geol. 529, 119293: DOI:
608 10.1016/j.chemgeo.2019.119293, 2019.
609 Li, K., Zhou, Y., Zhou, Q., Dong, Y., Zhang, Y., Chang, J., Chen, L., Lu, Y.:
610 Temporal-spatial distribution of euphotic depth and its influencing factors in
611 Lake Chenghai, Yunnan Province, China. J. Lake Sci. 31 (1), 256-267, DOI: 10.
612 18307 /2019. 0124, .2019
613 Li, Y., Chen, X., Xiao, X., Zhang, H., Xue, B., Shen, J., Zhang, E.: Diatom-based
614 inference of Asian monsoon precipitation from a volcanic lake in southwest
615 China for the last 18.5 ka. Quaternary. Sci. Rev. 182, 109-120, DOI:
616 10.1016/j.quascirev.2017.11.021, 2018.
617 Ling, Y., Sun, Q., Zheng, M., Wang, H., Luo, Y., Dai, X., Xie, M., Zhu, Q.:
618 Alkenone-based temperature and climate reconstruction during the last
619 deglaciation at Lake Dangxiong Co, southwestern Tibetan Plateau. Quatern. Int.
620 443, 58-69, DOI: 10.1016/j.quaint.2016.07.036, 2017.
621 Ljungqvist, F.C., Krusic, P.J., Sundqvist, H.S., Zorita, E., Brattström, G., Frank, D.:
622 Northern Hemisphere hydroclimate variability over the past twelve centuries.
623 Nature 532, 94-98, DOI: 10.1038/nature17418, 2016.
624 Lu Z., Study on climatic and environmental changes of the Yunnan Chenghai region
625 recorded bylake sediments since 1800 [D]. Kunming: The master Thesis of
626 Yunnan Normal University, 39-43, 2018.
627 MARGO Project Members: Constraints on the magnitude and patterns of ocean

cooling at the Last Glacial Maximum. Nature Geosci. 2, 127-132, DOI: 10.1038/ngeo411, 2009.

McManus, J.F., Francois, R., Gherardi, J.M., Keigwin, L.D., Brown-Leger, S.: Collapse and rapid resumption of Atlantic meridional circulation linked to deglacial climate changes. Nature 428, 834-837, DOI: 10.1038/nature02494, 2004.

Meegan Kumar, D., Woltering, M., Hopmans, E.C., Sinninghe Damsté, J.S., Schouten, S., Werne, J.P.: The vertical distribution of Thaumarchaeota in the water column of Lake Malawi inferred from core and intact polar tetraether lipids. Org. Geochem. 132, 37-49, DOI: 10.1016/j.orggeochem.2019.03.004, 2019.

Ning, D., Zhang, E., Shulmeister, J., Chang, J., Sun, W., Ni, Z.: Holocene mean annual air temperature (MAAT) reconstruction based on branched glycerol dialkyl glycerol tetraethers from Lake Ximenglongtan, southwestern China. Org. Geochem. 133, 65-76, DOI: 10.1016/j.orggeochem.2019.05.003, 2019.

Pearson, E.J., Juggins, S., Talbot, H.M., Weckstrom, J., Rosen, P., Ryves, D.B., Roberts, S.J., Schmidt, R.: A lacustrine GDGT-temperature calibration from the Scandinavian Arctic to Antarctic: Renewed potential for the application of GDGT-paleothermometry in lakes. Geochim. Cosmochim. Ac. 75, 6225-6238, DOI: 10.1016/j.gca.2011.07.042, 2011.

Pitcher, A., Hopmans, E.C., Mosier, A.C., Park, S.-J., Rhee, S.-K., Francis, C.A., Schouten, S., Sinninghe Damsté, J.S.: Core and Intact Polar Glycerol Dibiphytanyl Glycerol Tetraether Lipids of Ammonia-Oxidizing Archaea Enriched from Marine and Estuarine Sediments. Appl. Environ. Microb. 77, 3468, DOI: 10.1128/AEM.02758-10, 2011.

Powers, L., Werne, J.P., Vanderwoude, A.J., Sinninghe Damsté, J.S., Hopmans, E.C., Schouten, S.: Applicability and calibration of the $TEX_{86}$ paleothermometer in lakes. Org. Geochem. 41, 404-413, DOI: 10.1016/j.orggeochem.2009.11.009, 2010.

Powers, L.A., Werne, J.P., Johnson, T.C., Hopmans, E.C., Damsté, J.S.S., Schouten, S.: Crenarchaeotal membrane lipids in lake sediments: A new paleotemperature

658 proxy for continental paleoclimate reconstruction? Geology 32, 613-616, DOI:
659 10.1130/G20434.1, 2004.
660 R Development Core Team, R: A language and environment for statistical computing,
661 R Foundation for Statistical Computing, Vienna, Austria, 2013.
662 Rashid, H., Flower, B.P., Poore, R.Z., Quinn, T.M.: A ~25 ka Indian Ocean monsoon
663 variability record from the Andaman Sea. Quaternary. Sci. Rev. 26, 2586-2597,
664 DOI: 10.1016/j.quascirev.2007.07.002, 2007.
665 Reimer, P.J., Bard, E., Bayliss, A., Beck, J.W., Blackwell, P.G., Ramsey, C.B., Buck,
666 C.E., Cheng, H., Edwards, R.L., Friedrich, M.: IntCal13 and Marine13
667 radiocarbon age calibration curves 0–50,000 years cal BP. Radiocarbon 55,
668 1869-1887, DOI: 10.2458/azu_js_rc.55.16947, 2013.
669 Russell, J.M., Hopmans, E.C., Loomis, S.E., Liang, J., Sinninghe Damsté, J.S.:
670 Distributions of 5- and 6-methyl branched glycerol dialkyl glycerol tetraethers
671 (brGDGTs) in East African lake sediment: Effects of temperature, pH, and new
672 lacustrine paleotemperature calibrations. Org. Geochem. 117, 56-69, DOI:
673 10.1016/j.orggeochem.2017.12.003, 2018.
674 Saraswat, R., Lea, D.W., Nigam, R., Mackensen, A., Naik, D.K.: Deglaciation in the
675 tropical Indian Ocean driven by interplay between the regional monsoon and
676 global teleconnections. Earth. Planet. Sc. Lett. 375, 166-175, DOI:
677 10.1016/j.epsl.2013.05.022, 2013.
678 Schouten, S., Hopmans, E.C., Schefuß, E., Sinninghe Damsté, J.S.: Distributional
679 variations in marine crenarchaeotal membrane lipids: a new tool for
680 reconstructing ancient sea water temperatures? Earth. Planet. Sc. Lett. 204,
681 265-274, DOI: 10.1016/S0012-821X(02)00979-2, 2002.
682 Schouten, S., Hopmans, E.C., Sinninghe Damsté, J.S.: The organic geochemistry of
683 glycerol dialkyl glycerol tetraether lipids: A review. Org. Geochem. 54, 19-61,
684 DOI: 10.1016/j.orggeochem.2012.09.006, 2013.
685 Schouten, S., Rijpstra, W.I.C., Durisch-Kaiser, E., Schubert, C.J., Sinninghe Damsté,
686 J.S.: Distribution of glycerol dialkyl glycerol tetraether lipids in the water
687 column of Lake Tanganyika. Org. Geochem. 53, 34-37, DOI:

10.1016/j.orggeochem.2012.01.009, 2012.

Shen, C., Liu, K.-b., Tang, L., Overpeck, J.T.: Quantitative relationships between modern pollen rain and climate in the Tibetan Plateau. Rev. Palaeobot. Palyno. 140, 61-77, DOI: 10.1016/j.revpalbo.2006.03.001, 2006.

Sinha, A., Kathayat, G., Cheng, H., Breitenbach, S.F.M., Berkelhammer, M., Mudelsee, M., Biswas, J., Edwards, R.L.: Trends and oscillations in the Indian summer monsoon rainfall over the last two millennia. Nat. Commun. 6, DOI: 10.1038/ncomms7309, 2015.

Sinha, A., Stott, L., Berkelhammer, M., Cheng, H., Edwards, R.L., Buckley, B., Aldenderfer, M., Mudelsee, M.: A global context for megadroughts in monsoon Asia during the past millennium. Quaternary. Sci. Rev. 30, 47-62, DOI: 10.1016/j.quascirev.2010.10.005, 2011.

Sinninghe Damsté, J.S., Ossebaar, J., Abbas, B., Schouten, S., Verschuren, D.: Fluxes and distribution of tetraether lipids in an equatorial African lake: Constraints on the application of the $TEX_{86}$ palaeothermometer and BIT index in lacustrine settings. Geochim. Cosmochim. Ac. 73, 4232-4249, DOI: 10.1016/j.gca.2009.04.022, 2009.

Sinninghe Damsté, J.S., Ossebaar, J., Schouten, S., Verschuren, D.: Distribution of tetraether lipids in the 25-ka sedimentary record of Lake Challa: extracting reliable $TEX_{86}$ and MBT/CBT palaeotemperatures from an equatorial African lake. Quaternary. Sci. Rev. 50, 43-54, DOI: 10.1016/j.quascirev.2012.07.001, 2012a.

Sinninghe Damsté, J.S., Rijpstra, W.I.C., Hopmans, E.C., Jung, M.-Y., Kim, J.-G., Rhee, S.-K., Stieglmeier, M., Schleper, C.: Intact Polar and Core Glycerol Dibiphytanyl Glycerol Tetraether Lipids of Group I.1a and I.1b *Thaumarchaeota* in Soil. Appl. Environ Microb 78, 6866-6874, DOI: 10.1128/AEM.01681-12, 2012b.

Sun, W., Zhang, E., Shulmeister, J., Bird, M.I., Chang, J., Shen, J.: Abrupt changes in Indian summer monsoon strength during the last deglaciation and early Holocene based on stable isotope evidence from Lake Chenghai, southwest China.

718 Quaternary. Sci. Rev. 218, 1-9, DOI: 10.1016/j.quascirev.2019.06.006, 2019.
719 Tian, L., Wang, M., Zhang, X., Yang, X., Zong, Y., Jia, G., Zheng, Z., Man, M.:
720 Synchronous change of temperature and moisture over the past 50 ka in
721 subtropical southwest China as indicated by biomarker records in a crater lake.
722 Quaternary. Sci. Rev. 212, 121-134, DOI: 10.1016/j.quascirev.2019.04.003,
723 2019.
724 Tierney, J.E., Russell, J.M., Huang, Y., Damsté, J.S.S., Hopmans, E.C., Cohen, A.S.:
725 Northern Hemisphere controls on tropical southeast African climate during the
726 past 60,000 years. Science 322, 252-255, DOI: 10.1126/science.1160485, 2008.
727 Tierney, J.E., Russell, J.M., Eggermont, H., Hopmans, E.C., Verschuren, D., Damste,
728 J.S.S.: Environmental controls on branched tetraether lipid distributions in
729 tropical East African lake sediments. Geochim. Cosmochim. Ac. 74, 4902-4918,
730 DOI: 10.1016/j.gca.2010.06.002, 2010.
731 Wan, G.J., Chen, J.A., Wu, F.C., Xu, S.Q., Bai, Z.G., Wan, E.Y., Wang, C.S., Huang,
732 R.G., Yeager, K.M., Santschi, P.H.: Coupling between $^{210}Pb_{ex}$ and organic matter
733 in sediments of a nutrient-enriched lake: An example from Lake Chenghai, China.
734 Chem Geol 224, 223-236, DOI: 10.1016/j.chemgeo.2005.07.025, 2005.
735 Wang, H., Dong, H., Zhang, C.L., Jiang, H., Liu, Z., Zhao, M., Liu, W.: Deglacial and
736 Holocene archaeal lipid-inferred paleohydrology and paleotemperature history of
737 Lake Qinghai, northeastern Qinghai–Tibetan Plateau. Quaternary. Res. 83,
738 116-126, DOI: 10.1016/j.yqres.2014.10.003, 2015.
739 Wang, H., Dong, H., Zhang, C.L., Jiang, H., Zhao, M., Liu, Z., Lai, Z., Liu, W.: Water
740 depth affecting thaumarchaeol production in Lake Qinghai, northeastern
741 Qinghai–Tibetan plateau: Implications for paleo lake levels and paleoclimate.
742 Chem. Geol. 368, 76-84, DOI: 10.1016/j.chemgeo.2014.01.009, 2014a.
743 Wang, H., He, Y., Liu, W., Zhou, A., Kolpakova, M., Krivonogov, S., Liu, Z.: Lake
744 Water Depth Controlling Archaeal Tetraether Distributions in Midlatitude Asia:
745 Implications for Paleo Lake-Level Reconstruction. Geophys. Res. Lett. 46,
746 5274-5283, DOI: 10.1029/2019GL082157, 2019.
747 Wang, H., Leng, Q., Liu, W., Yang, H.: A rapid lake-shallowing event terminated

preservation of the Miocene Clarkia Fossil Konservat-Lagerstätte (Idaho, USA). Geology 45, 239-242, DOI: 10.1130/G38434.1, 2017a.

Wang, M., Tian, Q., Li, X., Liang, J., He, Y., Hou, J.: $TEX_{86}$ as a potential proxy of lake water pH in the Tibetan Plateau. Palaeogeogr. Palaeocl. 538, 109381, DOI: 10.1016/j.palaeo.2019.109381, 2020.

Wang, M., Zheng, Z., Man, M., Hu, J., Gao, Q.: Branched GDGT-based paleotemperature reconstruction of the last 30,000 years in humid monsoon region of Southeast China. Chem. Geol. 463, 94-102, DOI: 10.1016/j.chemgeo.2017.05.014, 2017b.

Wang, Q., Yang, X., Anderson, N.J., Zhang, E., Li, Y.: Diatom response to climate forcing of a deep, alpine lake (Lugu Hu, Yunnan, SW China) during the Last Glacial Maximum and its implications for understanding regional monsoon variability. Quaternary. Sci. Rev. 86, 1-12, DOI: 10.1016/j.quascirev.2013.12.024, 2014b.

Wang, S., Dou, H.: Lakes in China. Science Press, Beijing, China (in Chinese), 1998.

Weijers, J.W.H., Schouten, S., Spaargaren, O.C., Damste, J.S.S.: Occurrence and distribution of tetraether membrane lipids in soils: Implications for the use of the $TEX_{86}$ proxy and the BIT index. Org. Geochem. 37, 1680-1693, DOI: 10.1016/j.orggeochem.2006.07.018, 2006.

Wu, D., Chen, X., Lv, F., Brenner, M., Curtis, J., Zhou, A., Chen, J., Abbott, M., Yu, J., Chen, F.: Decoupled early Holocene summer temperature and monsoon precipitation in southwest China. Quaternary. Sci. Rev. 193, 54-67, DOI: 10.1016/j.quascirev.2018.05.038, 2018.

Wu, D., Zhou, A., Chen, X., Yu, J., Zhang, J., Sun, H.: Hydrological and ecosystem response to abrupt changes in the Indian monsoon during the last glacial, as recorded by sediments from Xingyun Lake, Yunnan, China. Palaeogeogr. Palaeocl. 421, 15-23, DOI: 10.1016/j.palaeo.2015.01.005, 2015.

Wu, J., Gagan, M.K., Jiang, X., Xia, W., Wang, S.: Sedimentary geochemical evidence for recent eutrophication of Lake Chenghai, Yunnan, China. J. Paleolimnol. 32, 85-94, 2004.

Yao, Y., Zhao, J., Bauersachs, T., Huang, Y.: Effect of water depth on the $TEX_{86}$ proxy in volcanic lakes of northeastern China. Org. Geochem. 129, 88-98, DOI: 10.1016/j.orggeochem.2019.01.014, 2019.

Yang, H., Xiao, W., Słowakiewicz, M., Ding, W., Ayari, A., Dang, X., Pei, H.: Depth-dependent variation of archaeal ether lipids along soil and peat profiles from southern China: Implications for the use of isoprenoidal GDGTs as environmental tracers. Org. Geochem. 128, 42-56, DOI: https://doi.org/10.1016/j.orggeochem.2018.12.009, 2019.

Zhang, E., Chang, J., Cao, Y., Sun, W., Shulmeister, J., Tang, H., Langdon, P.G., Yang, X., Shen, J.: Holocene high-resolution quantitative summer temperature reconstruction based on subfossil chironomids from the southeast margin of the Qinghai-Tibetan Plateau. Quaternary. Sci. Rev. 165, 1-12, DOI: 10.1016/j.quascirev.2017.04.008, 2017a.

Zhang, E., Chang, J., Shulmeister, J., Langdon, P., Sun, W., Cao, Y., Yang, X., Shen, J.: Summer temperature fluctuations in Southwestern China during the end of the LGM and the last deglaciation. Earth. Planet. Sc. Lett. 509, 78-87, DOI: 10.1016/j.espl.2018.12.024, 2019.

Zhang, E., Sun, W., Chang, J., Ning, D., Shulmeister, J.: Variations of the Indian summer monsoon over the last 30 000 years inferred from a pyrogenic carbon record from south-west China. J. Quaternary. Sci. 33, 131-138, DOI: 10.1002/jqs.3008, 2018.

Zhang, E., Zhao, C., Xue, B., Liu, Z., Yu, Z., Chen, R., Shen, J.: Millennial-scale hydroclimate variations in southwest China linked to tropical Indian Ocean since the Last Glacial Maximum. Geology 45, 435-438, DOI: 10.1130/G38309.1, 2017b.

Zheng, Y., Pancost, R.D., Naafs, B.D.A., Li, Q., Liu, Z., Yang, H.: Transition from a warm and dry to a cold and wet climate in NE China across the Holocene. Earth. Planet. Sc. Lett. 493, 36-46, DOI: 10.1016/j.epsl.2018.04.019, 2018.

807 **Figure captions**

808

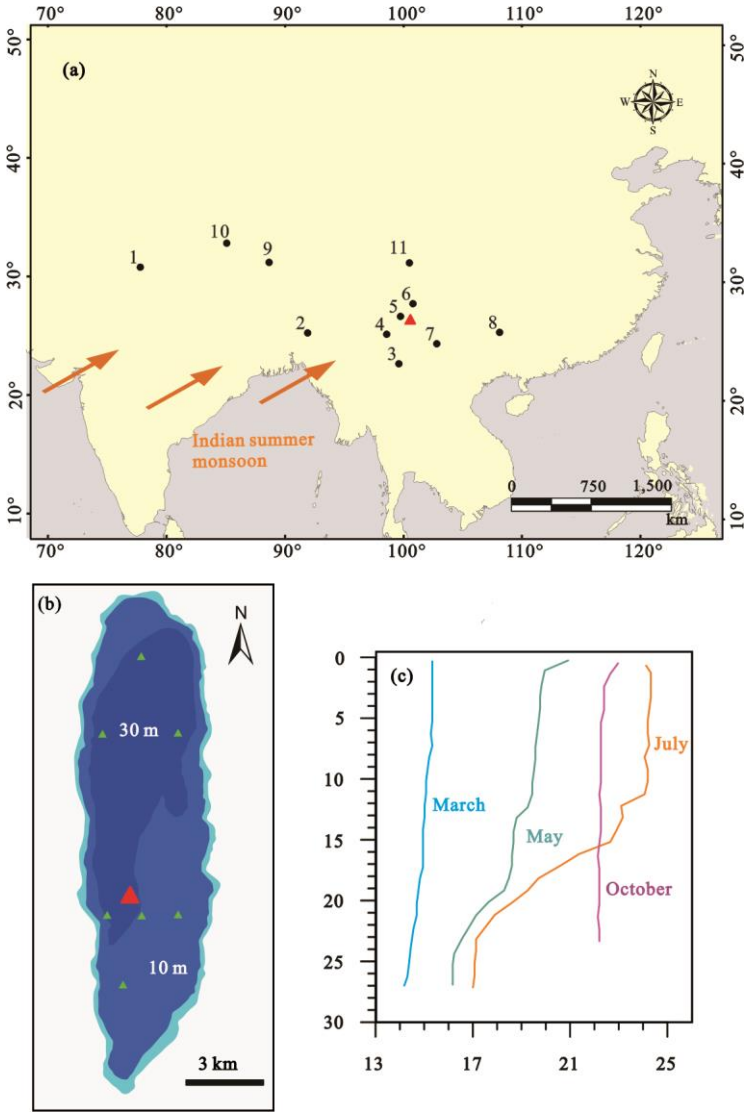


809

810 **Fig. 1.** (a) Map showing the location of Lake Chenghai in southwest China (red
811 triangle) and other sites (circles) mentioned in the text: 1. Bittoo Cave (Kathayat et al.,
812 2016); 2. Mawmluh Cave (Dutt et al., 2015); 3. Lake Ximenglongtan (Ning et al.,
813 2019); 4. Lake Tengchongqinghai (Zhang et al., 2017b; Li et al., 2018; Tian et al.,
814 2019); 5. Lake Tiancai (Zhang et al., 2017a, 2019); 6. Lake Lugu (Wang et al., 2014);
815 7. Lake Xingyun (Wu et al., 2015, 2018); 8. Dongge Cave (Dykoski et al., 2005); 9.
816 Nam Co (Günther et al., 2015); 10. Dangxiong Co (Ling et al., 2017); 11. Lake Yidun
817 (Shen et al., 2006), (b) The red triangle indicates the location of core CH2016 in Lake
818 Chenghai, while green triangles indicate the locations of surface samples. (c) The

vertical variation of Lake Chenghai water temperature in March, May, July and October (Lu, 2018).

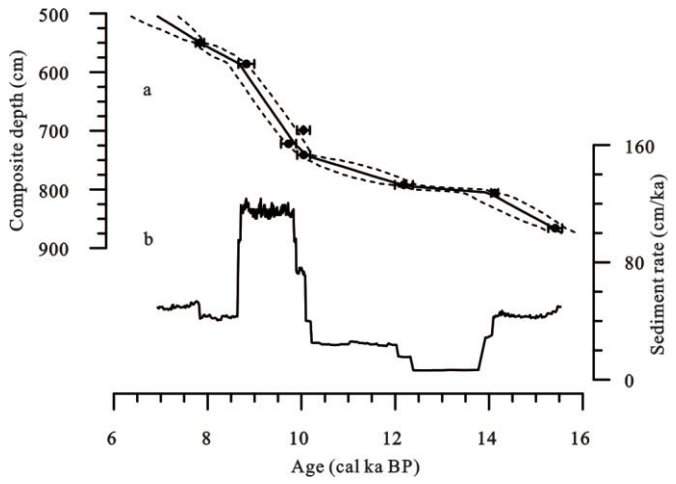


**Fig. 2.** (a) Age-depth model for the Lake Chenghai sediment core produced using Bacon software (Blaauw and Andres Christen, 2011) from Sun et al. (2019). Dotted lines indicate the 95% confidence range and the solid line indicates the weighted mean ages for each depth, error bars indicate the standard deviation range (2σ) of the calibrated radiocarbon dates. (b) estimated sedimentation rate (Sun et al., 2019).

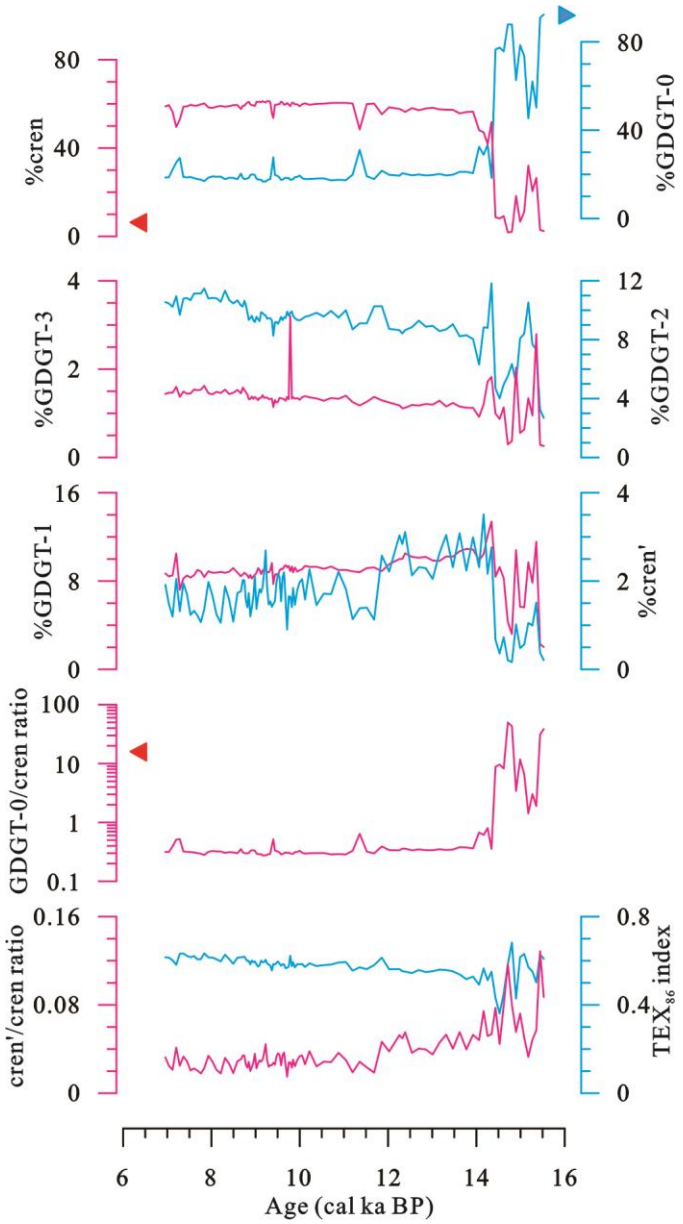


828

829 **Fig. 3.** Variations in the relative isoGDGT distribution and isoGDGTs-based proxies
830 of the Lake Chenghai sediment core. The triangles indicate the mean of surface
831 sediments.

832

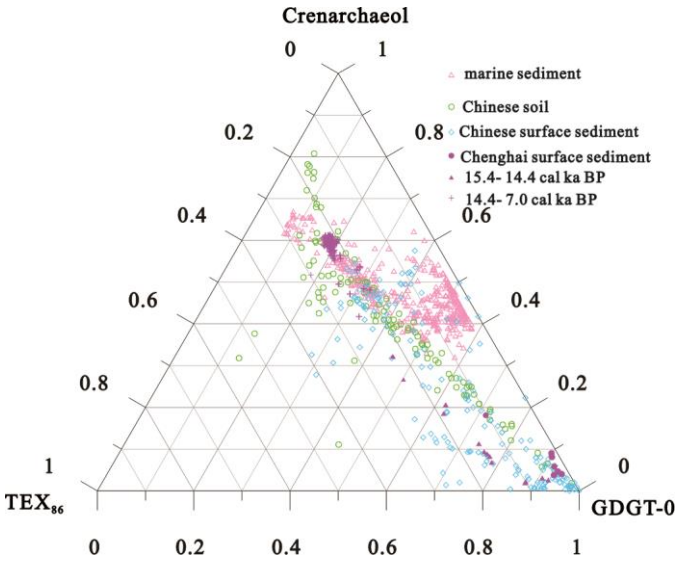


833

834 Fig. 4. Ternary diagram showing the distributions of GDGT-0, crenarchaeol, and
835 '$TEX_{86}$' GDGTs in surface and core sediments from Lake Chenghai, global marine
836 sediments (Kim et al., 2010), published Chinese soils compiled by Yao et al. (2019),
837 and lacustrine surface sediments (Günther et al., 2014; Dang et al., 2016; Hu et al.,
838 2016; Li et al., 2016, 2019; Yao et al., 2019; Wang et al., 2020).

839

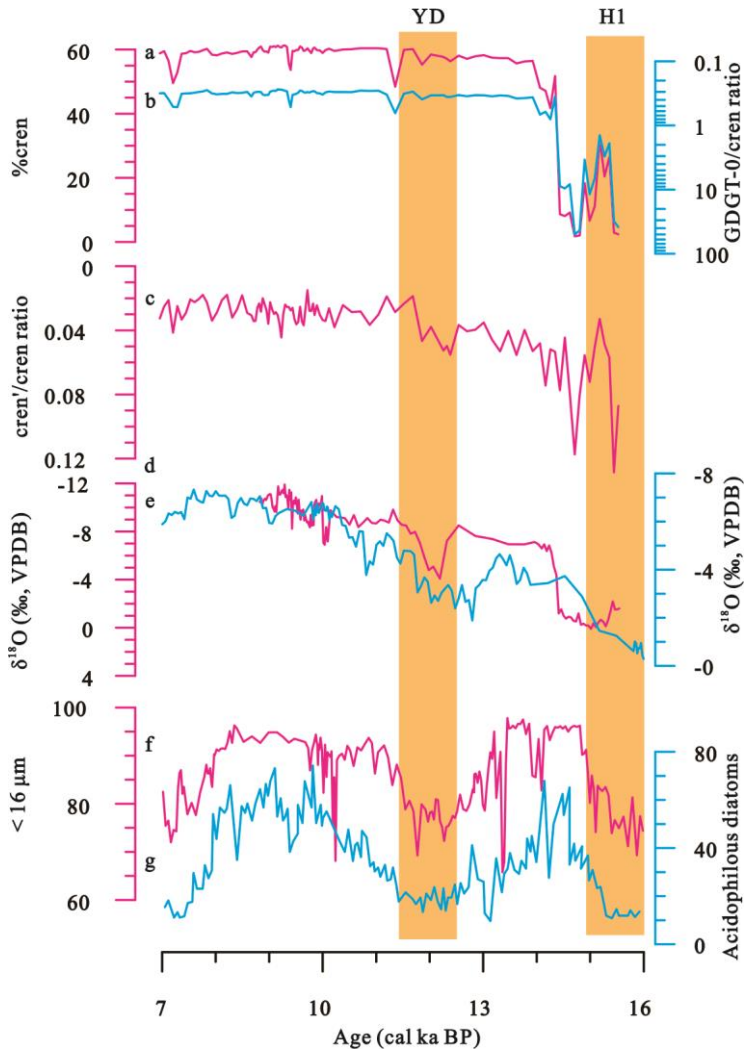


840

841 **Fig. 5.** Comparison of the isoGDGT-based lake-level record from Lake Chenghai (a-c)
842 with the $\delta^{18}O$ record of carbonate finer in grain size than 63 μm from Lake Chenghai
843 (d, Sun et al., 2019), the stalagmite $\delta^{18}O$ records from Mawmluh Cave in northeast
844 Indian (e, Dutt et al., 2015); grain-size and diatom record from Lake
845 Tengchongqinghai (f and g, Zhang et al., 2017; Li et al., 2018). The shading is utilised
846 to represent 'cold' events in the North Atlantic.

847

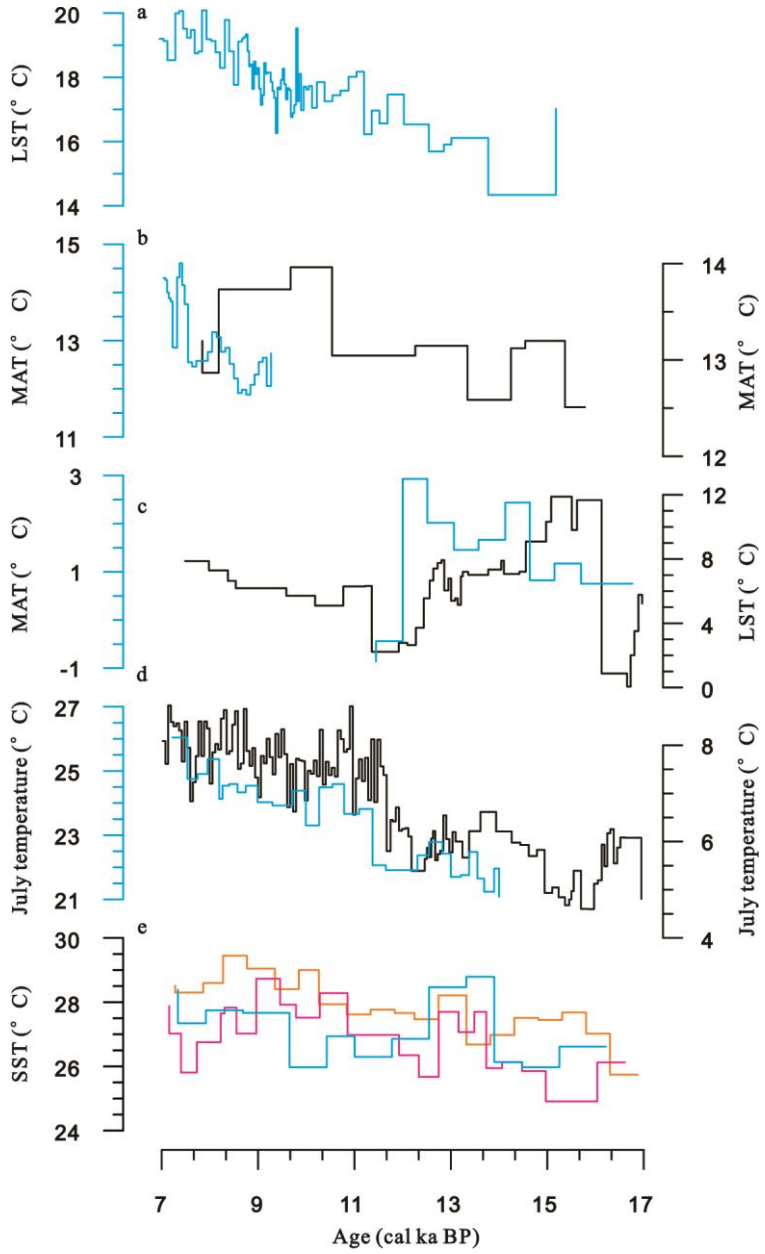


848

849 **Fig. 6.** A comparison of $TEX_{86}$-based lake surface temperature of Lake Chenghai (a)
850 with other paleotemperature records. (b) mean annual temperature based on branched
851 GDGTs from Lake Ximenglongtan (blue line, Ning et al., 2019) and Lake
852 Tengchongqinghai (black line, Tian et al., 2019); (c) Alkenone-based mean annual
853 temperature at Lake Dangxiong (blue line, Ling et al., 2017), and $TEX_{86}$-based lake
854 surface temperature of Nam Co from the southern Tibetan Plateau (black line,
855 Günther et al., 2015); (d) July temperature reconstructed from pollen record from
856 Lake Xingyun (blue line, Wu et al., 2018) and subfossil chironomids from Lake
857 Tiancai (black line, Zhang et al., 2017a, 2019);; and (e) sea surface temperatures in

858 the Andaman Sea and Bay of Bengal (Rashid et al., 2007; Govil and Naidu, 2011;
859 Gebregiorgis et al., 2016).
860